Comparison of Laser Induced Bulk Damage in Alkali-Halides at 10.6, 1.06, and 0.69 Microns

D. W. Fradin and Eli Yablonovitch*

Gordon McKay Laboratory, Harvard University
Cambridge, Mass. 02138

and

Michael Bass†

Raytheon Research Division
Waltham, Mass. 02154

It has long been recognized that catastrophic self-focusing cannot occur below a critical power P_c and that perturbations from self-focusing become progressively less important as the power of a probe optical beam is lowered below P_c. Using this fact, we have designed and conducted a number of experiments to study bulk damage in alkali-halides in which self-focusing was eliminated and unequivocal measurements of damaging fields obtained. Strongly focusing optical systems were used so that damage could be achieved while probe powers could be restricted to between one and two orders-of-magnitude below theoretical critical powers for electrostrictive self-focusing. Experimental evidence confirms the absence of self-focusing.

By observing the absolute magnitude of breakdown strengths and relative values among the alkali-halides, striking similarities between 10.6, 1.06 and 0.69 μm and d.c. avalanche breakdown were found. The results also showed no frequency dispersion over the wavelength range of 10.6 to 0.69 microns. The implications of this work for surface damage studies are explored, and, in addition, the effects of inclusions on bulk optical strength are considered.

Key Words: Alkali halides, avalanche breakdown, bulk damage, self-focusing, surface damage.

1. Introduction

Laser induced breakdown [1][1] in transparent dielectrics has been studied since high intensity optical fields have been available. Nevertheless, it has been difficult to ascertain the intrinsic bulk damage mechanism for these materials because of complications arising from self-focusing [2], multiphoton absorption and cascade ionization of impurities [3].

Recent work at 10.6 μm [4], however, indicates that intrinsic damage can be isolated. By choosing pure wide bandgap insulators, multiphoton ionization or its low frequency limit [5], tunnel ionization, can be eliminated. In addition, by confining laser powers to well below critical powers for self-focusing [6] catastrophic beam collapse becomes impossible and corrections from the index nonlinearity become quite small.

Supported by the Joint Services Electronics Program at Harvard University under Contract No. N00014-67-A-0298-0006.

Supported by the Advanced Research Projects Agency of the Department of Defense and was monitored by the Air Force Cambridge Research Laboratories under Contract No. F19628-70-0223.

Figures in brackets indicate the literature references at the end of this paper.

The alkali-halide family is a natural choice for breakdown studies. Besides being of practical importance for their application as optical materials in CO_2 lasers, they have large bandgap (about 7 ev or more) and have been studied extensively for both their d.c. dielectric strength [7] and their 10.6 μm characteristics [4].

The experimental studies reported here were conducted at 1.06 and 0.69 μm using Q-switched lasers. Since self-focusing may reach threshold before breakdown at these frequencies [8], it is important to understand both the conditions under which catastrophic self-focusing occurs and the corrections from the index nonlinearity when a catastrophic focus is prevented. For this reason an analysis of self-focusing is outlined in the appendices, and the general results relevant to our measurements are discussed in Section 3. Confirming theoretical predictions that catastrophic self-focusing is absent, two important experimental checks are then reported. We present in Section 4 the results of a series of carefully controlled experiments in which intrinsic bulk damage in alkali halides was measured. A well-characterized TEM_{00} mode laser beam with total power more than one order of magnitude below calculated critical powers for self-focusing was tightly focused within the samples in order to obtain the high intensities needed for damage. Then, in Section 5 we show how the experimental results can be fully explained in terms of avalanche breakdown.

2. The Lasers and Beam-Handling Optics

Figure 1 shows schematically the principal features of the laser damage source. The experiments were performed using a pulse pumped, electro-optically Q switched, Nd:YAG, or ruby laser. Some important properties of these devices are summarized in table 1. Figure 2 shows that the Nd:YAG laser output was in the lowest order Gaussian or TEM_{00} mode.

The time structure of the pulses from both lasers appears reasonably smooth when viewed with a fast photodiode oscilloscope combination having a measured risetime of 0.5 nsec. We have conducted Fabry-Perot studies on the ruby output and have found that normally fewer than four adjacent modes are oscillating simultaneously, so that at least with the ruby, the time structure is effectively fully resolved. Longitudinal mode selection is accomplished by aligning the faces of plane parallel laser rods parallel to the resonator mirror. Despite the low reflectivity of the anti-reflection coated rod surfaces, the high gain of the rod and the high reflectivity of the rear mirror create an effective resonant reflector.

To verify that the transverse mode structure on axis is constant with time, the centers of the beams were sampled with a 25-micron pinhole and found to have the same time structure as the entire beam. The stability on axis was found to be superior to stability of the spatially integrated power.

The breakdown data was taken by focusing through a ½-inch focal length lens to approximately 2 mm inside the samples. Care was taken to insure that spherical aberrations from both the lens and the plane entrance surface of the sample being tested were unimportant. A fast photodiode was used to monitor the transmitted light, and an energy monitor recorded the energy in each laser pulse.

Table 1. Laser parameters

	Nd:YAG	Ruby
Wavelength	1.06 μm	0.694 μm
Energy TEM_{00} Mode	1.5 mJ	2.0 mJ
Beam Diameter at Output Mirror TEM_{00} Mode	0.8 mm	0.7 mm
Polarization	Linear	Linear
Pulse Repetition Rate	1 pps	1 pulse/5 sec
Pulse Duration in TEM_{00} Mode	4.7 nsec (FWHP)	14 nsec (FWHP)
Pulse to Pulse Energy Reproducibility	± 7%	± 10%

The combination of one rotatable and one fixed polarizer resulted in a variable light attenuator which was highly sensitive, quite reproducible, and which did not affect the laser pulse's polarization, spatial distribution, or duration. If the fixed polarizer is oriented to transmit the laser polarization and if $\theta = 0^{o}$ is the angle of the rotating polarizer which gives maximum transmission through this attenuator, then the transmitted intensity at any other angle of rotation about the beam axis is

$$I(\theta) = bI_{o} \cos^{4}\theta \ .$$

I_o is the incident light intensity and b is the fraction transmitted when $\theta = 0^{o}$. Calibrated neutral density filters were often used in conjunction with the variable Glan attenuator.

3. Self-Focusing

A laser beam propagating in a transparent medium induces an increase in the index of refraction by an amount proportional to the laser intensity. At powers in excess of some critical power this nonlinearity causes the intensity distribution to become unstable, and a catastrophic beam collapse results.

Self-focusing may occur as the result of a number of nonlinearities. In solids for Q-switched laser pulses the process which normally leads to the smallest value of critical power and hence dominates self-focusing is electrostriction [10]. This is the case for the alkali halides where thermal and electronic contributions to self-focusing are much smaller than the electrostrictive effect [11] and can be neglected.

An intense light wave whose power lies below a critical power P_c will not experience a catastrophic collapse in a nonlinear medium, because although focusing by self-action will always be present, diffraction acts in the opposite sense to cause divergence and dominates at such powers [10]. At powers sufficiently far below P_c, therefore, the intensity distortion due to the index nonlinearity can be treated as a constant perturbation on diffraction effects and usually neglected. These observations allow us to effectively eliminate self-focusing by restricting probe powers to well below calculated critical powers while focusing strongly by external optics to reach the field intensities necessary to cause optical damage.

Theoretical self-focusing parameters are defined and derived in the appendices where quantitative corrections from the index nonlinearity at powers below P_c are discussed. Table 2 summarizes the numerical results. The probe power is the experimental peak power on axis and is more than one order of magnitude below P_c. From a purely theoretical viewpoint, therefore catastrophic self-focusing is impossible, and it can be shown that beam distortion from the index nonlinearity introduces at most a few percent correction in the measured electric field strengths. If catastrophic self-focusing does occur, then the breakdown damage data is a measure of the critical powers rather than intrinsic breakdown field. The measured threshold intensity will then scale with the square of the calculated focal diameter if the process is steady-state and will depend on the pulse-width if the process is transient. (The diameter dependence in the steady-state results from the existence of a constant critical power P_c which does not vary with beam diameter.)

Table 2. Calculated steady-state, self-focusing parameters and experimental values of pulse-width and peak power

	Wavelength (microns)	τ (10^{-9} sec)	t_p (10^{-9} sec)	$n_2 \times 10^{22}$ (mks)	P_{cr} (10^3 watts)	P_c (10^3 watts)	P_{probe} (10^3 watts)
	10.6*	11.0	200		48,000	175,000	120
NaCl	1.06	5.3	4.7	2.3	480	1,750	37.8
	0.69	3.94	14		204	746	20
	10.6*	22.3	200		13,200	50,000	20
RbI	1.06	10.7	4.7	8.4	132	500	6.1
	0.69	8.0	14		56	203	--

For $P_{probe} < P_c$ catastropic self-focusing will not occur.

* The 10.6 μm data is taken from E. Yablonovitch, Appl. Phys. Letters 19, 495 (1971).

To test our belief that self-focusing was absent we conducted two experiments. In the first the relative field strength threshold for damage in NcCl was measured with three different focusing lenses, corrected for spherical aberrations, and having focal lengths of 0.5, 1.0, and 1.5 inches. The experiment was conducted at 1.06 μm. If steady-state self-focusing were present, the observed damage threshold would have scaled with the inverse of the focal length. It did not, and, in fact, to within 5 percent the field strength was independent of focal length. This effectively eliminated the possibility of steady-state self-focusing. Since t_p/τ was just under unity, however, self-focusing could be transient, and equation (A15) predicts the results observed. For this reason it was necessary to measure the damage threshold as a function of pulse width with the beam diameter held essentially constant.

By changing the pumping level for the YAG laser, we were able to extend the pulse width by a factor of 2.3 to 10.8 nsec. In addition, the breakdown strength at 0.69 μm was measured with ruby laser pulses of 14-nanosecond duration and a focused diameter 25 percent smaller than that obtained with the YAG laser. the same ½-inch focal length lens was used in all three measurements, and to compute the ruby value, we assumed the same transverse intensity variation as that present at 1.06 μm. To within 15 percent no change was noted in the threshold field despite the pulse-width dependence in eq (16). The agreement for the ruby pulses was especially reassuring, because the critical power varies with wavelength squared. If transient self-focusing were present, we would have seen a change by a factor of 4.2 in the field strength or a factor of 18 in the measured intensity--an effect which would have been quite dramatic. A factor of 9 comes from the pulse-width dependence of the transient critical power and a factor of 2 from the wavelength dependence.

Perhaps the best experimental check for self-focusing is the actual measurement of breakdown strengths. Self-focusing theory appears to be totally unable to account for the experimental results given below in which both relative and absolute values of breakdown strengths show striking similarities to 10.6 μm values. We thus conclude that prior to the onset of material damage, self-focusing has been effectively eliminated as a competing nonlinearity.

The possibility may exist that self-focusing by a mechanism other than electrostriction will be effective after a sufficient number of electrons have been generated to cause intense local heating of the sample. Evidence for such an effect has been observed with gas breakdown [12], but the results are not entirely unambiguous. While theoretical arguments can be given against such an effect, it is sufficient to note that our experimental findings indicate that any late developing nonlinearity is unimportant in our measurements.

4. Experimental Measurements of Breakdown

4.1 Damage Measurements at 1.06 Microns

To measure the breakdown strengths of the alkali halides, we focused the laser beam approximately 2mm into each sample and recorded the number of laser pulses necessary to produce internal damage at various power levels. In every case where damage occurred, a white spark was produced, and the damage was later carefully inspected with a microscope. Because of the small volume damaged by our highly focused 1.06 μm pulses (less than $2 \times 10^{-5} mm^3$), a large number of data points could be taken with each sample (40 to 100).

Defining threshold as that value of incident power necessary to produce intrinsic damage in a single shot for 50 percent of the positions probed [4], we calculated the r.m.s., on-axis electric field at the measured threshold in NaCl. Corrections were made for reflections from various surfaces and the changes in the beam diameter due to the effect of the index nonlinearity. This was the basic calibration, and all other values of threshold were measured relative to E_{NaCl}. In order to avoid errors from daily power fluctuations and possible alignment changes, a single sample of NaCl was tested with each alkali halide. It was readily determined that a slight misalignment of the focusing lens (½-inch focal length) had no measurable effect on the relative breakdown strengths.

Visual inspection and the breakdown statistics suggested that spatial inhomogeneities from inclusions were not affecting the results except in the single case of RbCl. Damage which we regarded as intrinsic consisted at each damage position of a single pointed region which began at the geometrical focus and extended a very short distance back toward the laser, increasing in cross-section to give a tear-drop appearance. A typical example is indicated in figure 3. In RbCl, on the other hand, regions with low breakdown thresholds consisted typically of one or more spherical voids randomly distributed about the focus (figure 4). A number of points, however, did appear visually to have intrinsic damage and were consistently more difficult to breakdown. These data points were used for the RbCl results.

Finally, a fast photodiode detector system with a 0.5 nsec risetime monitored the transmitted light as shown in figure 5 and was used to confirm threshold levels in NaCl and KCl as well as to establish the approximate time structure and stability of the laser output.

Values for the breakdown field obtained at 1.06 μm are summarized in figure 6 and in table 3 along with both the 10.6 μm data collected by Yablonovitch [4] and accepted d.c. results [9]. These results are normalized to the respective values of field necessary to damage NaCl. The breakdown fields for NaCl are listed in table 4. This allows the striking similarity in trend of breakdown field to be easily observed and the possible systematic deviations at 1.06 μm to be easily recognized. The quoted errors at 10.6 μm are ± 10 percent, and our random experimental errors in relative fields are estimated to be no more than ± 10 percent with possible errors due to microscopic strains adding another ± 5 percent. For NaCl and KBr two different samples from two different manufacturers gave nearly identical results.

Table 3. Relative breakdown fields - normalized to $E_{NaCl} \approx 2 \times 10^6$ V/cm

	NaI	NaBr	NaCl	NaF
DC	0.460	0.553	1	1.60
10.6 μm	0.405	0.476	1	----
1.06 μm	(0.293)*	0.675	1	1.78
	KI	**KBr**	**KCl**	**KF**
DC	0.380	0.460	0.667	1.27
10.6 μm	0.369	0.482	0.713	1.23
1.06 μm	0.272	0.375	0.568	----
	RbI	**RbBr**	**RbCl**	
DC	0.327	0.387	0.553	
10.6 μm	0.323	0.400	0.472	
1.06 μm	0.400	0.550	0.670	

*Crystal was extremely hydroscopic and no final check was made with the microscope to determine if inclusions were responsible for the damage observed.

Table 4. Absolute breakdown strength of NaCl

E_{peak}(dc)	1.50×10^6 V/cm	
E_{rms}(10.6 microns)	1.95×10^6 V/cm	± 10 Percent
E_{rms} (1.06 microns)	2.3×10^6 V/cm	± 20 Percent
E_{rms}(0.69 microns)*	2.2×10^6 V/cm	± 20 Percent

* Gaussian profile assumed.

A 4 percent correction is incorporated into the 0.69 micron value because of equation (A12) in the text. The data at 1.06 microns, however, is transient as seen from table 2. Equation (A15) is therefore used to evaluate P_{cr} and a 1.8 percent correction determined from (A12).

Careful statistics for variations in the breakdown strength were collected on NaCl because of the high quality of the two samples we obtained. It was found that, accounting approximately for experimental uncertainties, the process appeared threshold-like. For the other samples larger fluctuations were noticed, but the sample qualities were somewhat inferior to that of NaCl. Experimental uncertainties are considered to result from surface imperfections, internal strains, and laser fluctuations. No measurement of any probabilistic nature to breakdown was made.

Some evidence for intrinsic fluctuations, however, was found by monitoring the light transmitted through the samples. On several occasions a laser pulse produced damage in the same position where a more intense pulse one second before had been focused without damaging the sample. While these observations may have resulted from unresolved time-structure in the second laser pulses, the same observations

were made at ruby wavelength where Fabry-Perot studies indicated that the pulses were normally free of such fluctuations.

4.2 Damage Measurements at 0.69 μm

The breakdown strength of NaCl was also measured with a ruby laser. Table 4 records the average of about 50 damage measurements. Although the laser was normally operating in a single longitudinal mode as indicated by Fabry-Perot and photodiode studies, each laser shot during the measurement was monitored with a fast photodiode and recorded.

In figure 7 time-resolved photographs of transmitted light indicate the sudden attenuation normally seen for laser pulses which caused damage. Because of the smooth time-structure of most of the pulses, we are able to record a few cases in which the instant of first attenuation, considered to be the onset of material damage, occurred after the peak of the laser pulse had passed. An example is given in figure 7c. The same effect was observed at 1.06 μm. This may be explained both by invoking a statistical model for breakdown [13] or by the considerations of a time-dependent avalanche discussed in the next section.

5. Discussion of Results

5.1 Bulk Damage

The experiments reported here were performed under carefully controlled conditions using stable, well-characterized lasers and optical systems for which aberrations were unimportant. Because we were able to probe each sample in many different positions, random fluctuations in breakdown strength were averaged out. It was possible to distinguish between inclusion and intrinsic damage by inspection of the residual damage and to correct for the effects of inclusions in the one material for which they were important. In addition, experimental tests showed that catastrophic self-focusing was absent and, consistent with theory, that the index nonlinearity did not affect the results to within experimental error. It is therefore concluded that the results of the 1.06 and 0.69 μm study as summarized in figure 6 and table 4 represent accurate measurements of intrinsic bulk damage.

Because the techniques of this study are virtually identical to those of reference 4, direct comparison can be made to breakdown strengths at 10.6 μm. It has already been observed that the damage thresholds for the alkali-halides at 1.06 μm follow a trend nearly identical to that observed with the CO_2 laser and, in fact, to the d.c. measurements of reference 9. It thus appears that the intrinsic process of laser-induced damage for the alkali-halides has the same fundamental character as both a.c. damage in the infrared and d.c. avalanche breakdown. Moreover, the consistency of the absolute breakdown strengths at 0.69 μm suggests that this same process dominates at frequencies as high as 4.3×10^{14} hertz.

Additional support for an avalanche mechanism comes from three experimental observations concerning the time-structure of the laser probe pulses. The first is that increasing the pulse-width of the YAG laser output by a factor of 2.3 resulted in a 14 percent average drop in threshold intensity for NaCl. Averages were taken at about 20 shots at each pulse width. This change, though small, is probably real, because the test was made on a single sample of high-quality NaCl and thereby avoided a major source of experimental uncertainties arising from material variations. The second observation, noted at both 1.06 and 0.69 μm, is that high-frequency time-structure on the pulse has little measurable effect on the breakdown strength. And finally, after adjusting the power level so that damage occured regularly near the top of the laser pulses, the probe intensities were increased by a factor of about three by changing the beam attenuation. When this was done, the intensity at which the transmitted light dropped (cf. figure 7) was higher by 15 percent or more than it had been with the lower intensity pulses. This was determined to mean that increasing the effective risetime of the optical field raises the measured breakdown strength. To understand both this set of observations and the results from table 4, some discussion of existing electron avalanche theories [7, 14] is given.

An electron avalanche in solids is a rapid multiplication of conduction-band electrons in which an initially low density N_o of free carriers interacts with an intense electric field in the presence of phonons. When the electric field reaches a critical value, the number of electrons increases with time approximately as

$$N(t) = N_o \exp \left[\int_o^t \alpha(E) dt \right] .$$

The gain coefficient $\alpha(E)$ is a strongly varying function whose value can be inferred from d.c. measurements of breakdown strength as a function of sample thickness for extremely thin specimens [15]. Lattice disruption then results from joule heating.

Two important conclusions develop from such an analysis. The first is that the entire process of avalanche and damage involves energy exchange between the field and the material which is approximately described by the well-known formula for a.c. conductivity

$$\frac{dW}{dt} = \frac{Ne^2\tau}{m(1 + \omega^2\tau^2)} E^2 \qquad (1)$$

where N is the time-dependent electron density, ω the angular frequency, and τ the characteristic relaxation-time determined principally from phonon collisions. While this precise form of the conductivity may not be correct for polar materials such as the alkali-halides, we will use it to qualitatively describe breakdown for high frequencies.

Because of eq (1), energy input to the material scales with frequency and field as $E^2/(1 + \omega^2\tau^2)$, and because the details of energy input determine the electron distribution function and hence N(t), the threshold for damage will scale in the same manner. This justifies the use of root-mean-square fields in table 4. It also indicates that the a.c. breakdown strength will increase for frequencies near $1/\tau$. Calculation of τ for NaCl [15] indicates that frequency dispersion should begin to occur somewhere near that of the ruby laser.

The second relevant conclusion from an analysis of avalanche breakdown is that if insufficient time exists for the electron density to reach values necessary to damage, then damage will not occur even though electron recombination losses have been exceeded and an electron avalanche is underway. Damage will only be produced when the field is subsequently raised above the steady-state breakdown strength and the gain coefficient α is correspondingly increased. Such an effect has been observed in d.c. experiments by varying the duration of constant applied fields [16] and by measuring threshold fields for samples of thickness less than about 100 μm [17], where transit effects limit the build-up time. When the time available for the build-up of the avalanche is reduced below about 50 ns, larger fields are needed to damage.

The exerpiments of reference 16 give a useful comparison to our work. It was found that when the applied d.c. field duration was reduced to 10 ns, the breakdown strength of NaCl increased to 2.1×10^6 volts/cm. Because our laser pulses had durations of about 10 ns, the discrepancy in absolute field strengths between optical and d.c. measurements may be fully explained. In addition, the field dependence of $\alpha(E)$ in NaCl is qualitatively correct to explain our observations of the pulse-width dependence to breakdown, the insensitivity of threshold to fast-time structure, and the increase in breakdown strength for rapidly rising pulses. It also indicates that when approximate corrections from pulse-width considerations are made and experimental uncertainties ignored, the ruby laser threshold is a few percent greater than the threshold at 1.06 μm.

The essential details of the breakdown studies reported here are thus fully explained by the process of avalanche breakdown.

5.2 Implications For Surface Damage Studies

Surface damage is often a practical problem in the operation of high-power lasers. For this reason a number of investigations of surface breakdown [13, 18], have been made with the aim of elucidating the conditions and mechanisms of surface damage. The techniques of the studies reported here may provide a valuable tool for understanding surface damage by allowing direct comparison to bulk damage thresholds. This comparison can be made by focusing a low-power laser beam first on a surface and then about 2 mm into the bulk. Because focusing problems are much less severe in the bulk and damage from inclusions can apparently be distinguished by visual observation, a stable and repeatable reference exists for surface studies. Careful investigation should help elucidate, in particular, the mechanisms responsible for surface damage under various conditions of surface preparation.

6. Conclusions

Careful measurements of laser-induced bulk damage have been made in ten alkali-halides without the confusing effects of self-focusing. Comparison of the results to studies at d.c. and 10.6 μm indicated that the process of a.c. avalanche breakdown, similar in fundamental character to d.c. avalanche breakdown, is responsible for the damage observed. Analysis of time-related observations confirm this conclusion.

7. Acknowledgments

The skillful assistance and advice of D. Bua and S. Maurici are gratefully acknowledged. We are also indebted to Prof. N. Bloembergen for valuable discussions of breakdown theory.

8. Appendix A

To demonstrate the claim that the relative balance between diffraction and self-focusing effects is set at the entrance plane for a general steady state nonlinearity, we calculate the curvature of the ray path from a modified, eikonal equation formalism that incorporates both diffraction effects and the steady-state nonlinearity [19]. Its applicability is restricted to beams with diameters 2a much less than a wavelength -- a condition fulfilled in our experiments.

Writing the electric field vector $\vec{E}(\vec{r})$ as $\vec{A}(\vec{r})$ exp i [$k_o \phi(r)$ - wt] where $k_o = w/c$ and the index nonlinearity is $n_2 A^2$ and ignoring terms of order $n_2 A^2/n_o$, we can write Maxwell's equations in the simplified form

$$[(n_o + n_2 A^2)^2 - (\text{grad } \phi)^2]\ \vec{A} + \frac{1}{k_o^2}\ \nabla^2 A = 0 .$$

If the scalar product of this equation is taken with $\vec{A}$, a term containing the factor $1/k_o^4$ dropped and a cross term with $n_2 A^2$ neglected, this leads directly to an effective eikonal equation

$$n_1^2 - (\text{grad } \phi)^2 = 0 \qquad (A1)$$

where

$$n_1 = n_o + n_2 A^2 + \frac{1}{2k_o^2 n_o} \frac{\nabla^2 A}{A} . \qquad (A2)$$

In the limits of zero nonlinearity, and infinitesimal wavelength, this is just the basic equation of geometrical optics. Results derived from the usual eikonal equation [20] can now be used with the index of refraction replaced by eq (A2). In particular, the curvature $d^2\vec{r}/d\rho^2$ for a pencil of rays with position vector $\vec{r}$ and with ρ the coordinate along the ray path is given by

$$d^2\vec{r} = \frac{1}{n_1} [\text{grad } n_1 - \frac{dn_1}{d\rho} \frac{d\vec{r}}{d\rho}] \qquad (A3)$$

Equation (A3) can be simplified by restricting the treatment to cylindrically symmetric beams and by assuming that the maximum ray slope is small compared to unity. (In our experiments the maximum slope inside the sample and before the focus is less than 0.05.) Both the second term on the right in eq (A3) and the longitudinal component of the Laplacian in eq (A2) are negligible. The curvature is now expressed in a form first derived by Talanov [21].

$$\frac{d^2\vec{r}}{d\rho^2} \approx \frac{d^2\vec{r}}{dz^2} = \frac{1}{n_1} \text{grad}_\perp n_1 .$$

This result is important to the study of self-focusing effects because the sign of $d^2\vec{r}/dz^2$ indicates whether or not the beam is converging and its magnitude is a quantitative measure of that convergence or divergence. A positive curvature results in an increase in the slope of the ray path with respect to the propagation direction and thus represents a divergence from the axis. Diffraction alone will produce a positive curvature in an isotropic medium. A negative curvature, on the other hand, will cause convergence of the beam towards the axis and indicates the dominance of the self-focusing nonlinearity.

$A^2(r)$ is proportional to the light intensity, and where the beam propagates with little or no change in shape, the intensity is equal to the power in the beam divided by the beam area $\pi a^2(z)$. Let p be an effective power which absorbs these proportionality constants including the factor π in the beam area. This effective power has, in fact, a functional form -- it may be Gaussian (exp [- $2r^2/a^2$]) for example -- and it is this functional form which describes the beam shape. We can therefore consider p to be a function of a radial variable which is independent of beam size. Defining the coordinate x as x = r/a(z), we can write

$$A^2(r) = \frac{p(x)}{a^2(z)} = \frac{\text{effective power}}{\text{beam area}} \qquad (A5)$$

Equation (A5) is normally assumed in numerical calculations and has been referred to as the "constant shape approximation" [22]. Along with eq (A4) it provides the basic relationships to calculate the critical power, the self-focusing length, and the quantitative influence of the index nonlinearity when diffraction dominates.

By expanding $\nabla_\perp^2$ in cylindrical coordinates r and z it is easily seen that $\nabla_\perp^2 A/A$ is also proportional to a^{-2}. We can then write eq (A2) as

$$n_1 = n_0 + \frac{1}{a^2(z)} f(x)$$

where f(x) is the sum of contributions from both diffraction and the index nonlinearity. Since $\text{grad}_\perp$ is just $a(z)^{-1}[\partial/\partial x]$, and since n_1 in the denominator of eq (4) can be replaced by n_o, the derivative of f(x), which contains no dependence on z, determines the relative importance of diffraction and self-focusing. Once this relative importance is determined for one value of z, such as z = 0 at the entrance plane, it is determined for all z.

For completeness we write eq (A4) in the final form

$$\frac{d^2 r}{dz^2} = \frac{1}{n_o} \frac{1}{a^3(z)} \frac{d}{dx}[f(x)] \tag{A7}$$

where, using (A5),

$$f(x) = n_2(aA)^2 + \frac{1}{(2A)}\left[\frac{d^2(aA)}{dx^2} + \frac{1}{x}\frac{d(aA)}{dx}\right] \tag{A8}$$

The importance of neglected terms can be determined for a particular beam shape and has been shown to be negligible [19] except near a catastrophic self-focus or under experimental condition where extreme external focusing is used.

The critical power P_c is in principle calculated from the requirement that the derivative f(x) vanish for all x, leading to a detailed balance of self-focusing and diffraction. Since f(x) contains no dependence on beam diameter, the critical power will not be dependent on beam diameter for a steady-state nonlinearity.

Appendix B

The index nonlinearity leads to intensity distortions even below the critical power for catastrophic self-focusing. Using the results of Appendix A quantitative corrections from the nonlinearity can be derived.

In eq (A7) r is replaced by x a(z) and a new function g(x) defined. This gives

$$\frac{d^2 a}{dz^2} = \frac{1}{a^2(z)} g(x) \tag{A9}$$

where

$$g(x) = \frac{1}{n_o x} \frac{d}{dx} f(x). \tag{A10}$$

eq (A9) is multiplied by dz(da/dz) and integrated, we find

$$\left(\frac{da}{dz}\right)^2 = - \frac{g(x)}{a^2} + c\,. \tag{A11}$$

Considerable simplifications results from expanding A^2 and therefore g(x) about small x and retaining terms to order x^2. In reference 2 this expansion is carried out for a Gaussian beam. We can investigate the geometrical focus at low powers by setting the derivative in eq (A11) equal to zero [6]. After some manipulation the focal diameter d is evaluated in terms of d_o, the diameter in absence of a nonlinearity. In particular,

$$d = d_o(1 - P/P_{cr})^{\frac{1}{2}} \tag{A12}$$

where P is the full power in the beam and P_{cr} is given in cgs units by

$$P_{cr} = \frac{c\lambda^2}{32\pi n^2} \tag{A13}$$

The result (A12) is useful for P/P_{cr} less than about 0.5. The calculated on-axis intensity at breakdown must be multiplied by a factor $(d_o/d)^2$ to approximately correct for the effects of the nonlinearity.

More extensive analysis shows that P_{cr} is the critical power for self-focusing near the center of a Gaussian beam [22]. For input powers greater than P_{cr} but less than P_c, diffraction dominates everywhere except near the beam center. A collimated beam will initially intensify at such powers until the diffraction of the wings causes the on-axis intensity to drop. P_{cr} differs from P_c because the latter is a quantity averaged over the entire beam while P_{cr} is determined by the behavior near the center. In fact, P_c is not a precisely defined quantity because it is not possible to exactly balance diffraction and self-focusing over the entire beam cross-section. At an input power of P_c, therefore, a propagating beam will not change its size measurably and so not experience a catastrophic self-focus, but its intensity distribution will be distorted. P_c has the same functional form as P_{cr} and differs by just a numerical factor as $P_{cr} = 0.273\ P_c$ for Gaussian beams.

Appendix C

The analysis of Appendix A and the results derived from it are correct only in the steady state. In solids the dominant nonlinearity is normally electrostriction, and if the process is transient, it is no longer true that the relative balance between diffraction and self-focusing is independent of propagation distance and that the critical powers are independent of beam diameter. The changes occur because electrostriction becomes non-local in both a temporal and a spatial sense. Although a susceptibility approach such as we have used is no longer strictly correct, it is nonetheless useful for establishing functional dependences for self-focusing parameters and approximate quantitative values.

For our experiments two results from a transient analysis are important [23]. The first is that transient effects decrease the effective nonlinear index n_2 and thus make self-focusing more difficult. If we wish to avoid self-focusing by restricting our powers to well below the critical power, the steady-state analysis gives us a lower bound on P_c. Being in a transient regime can, therefore, only increase our margin of safety and improve the accuracy of our experiment by making the corrections indicated by eq (A12) less important.

The second important result involves the dependence of the critical power on laser pulsewidth and on beam diameters. In the steady state the nonlinear index n_2 is given by [10]

$$n_2 = \frac{n_o\left(\rho \frac{\partial n_o}{\partial \rho}\right)^2}{4\pi\rho v^2}$$

where n is the index of refraction in the absence of the nonlinearity, ρ is the material density, and v is the acoustical sound velocity. The quantity $(\rho\ \partial n_o/\partial\rho)$ for cubic materials such as the alkali-halides may be found approximately by differentiating the Clausius-Mosotti equation. The remaining constants are tabulated in handbooks.

When the laser pulse width t_p is shorter than the electrostrictive response time $\tau = a/v$, n_2 is decreased in value, thereby increasing the critical power. For a triangular pulse, Kerr [13] has shown that

$$(n_2)_{transient} = (n_2)_{steady\text{-}state}\left[1 - \frac{a}{v\rho} D\left(\frac{v\rho}{a}\right)\right] \tag{A14}$$

where $D(\frac{v\rho}{a})$ is Dawson's integral with

$$D(\xi) = \exp(-\xi) \int_0^{\xi} \exp \eta^2 d\eta .$$

When $t_p \lesssim \tau/2$,

$$(n_2)_{\text{transient}} \approx k(n_2)_{\text{steady state}} \frac{v^2 t_p^2}{a^2} .$$

This result is valid for more general and realistic pulse-shapes with the numerical constant k being of order unity and having a value dependent on the precise time-structure of the pulse. When this result is inserted into eq (A13), the critical power becomes

$$P_{c_{t_p/\tau \lesssim \frac{1}{2}}} = (P_c)_{\text{steady state}} \frac{a^2}{kv^2 t_p^2} . \qquad \text{(A15)}$$

For short laser pulses, therefore, there exists more properly a critical intensity rather than a critical power, and in this transient regime fairly small changes in pulse-width will have a significant effect on the critical power.

9. References

[1] Zverev, G. M. et al., Zh. Eksp. Teor. Fiz. 53, 1849 (1967) [Sov. Phys. JETP 26, 1053 (1968)].

[2] Akhmanov, S. A. et al., Usp Fiz Nauk. 93, 19 (1967) [Sov. Phys. Uspekhi 10, 609 (1968)].

[3] Hellwarth, R. W., in Damage in Laser Materials, edited by A. J. Glass and A. H. Guenther, NBS Spec. Publ. 341 (U.S. Dept. of Commerce, Wash., D.C., 1970), p. 67.

[4] Yablonovitch, E. Appl. Phys. Lett. 19, 495 (1971).

[5] Keldysh, L. V., Zh. Eksp. Teor. Fiz. 47, 1945 (1964) [Sov. Phys. JETP 20, 1307 (1965)].

[6] Zverev, R. M. and Pashkov, V. A., Zh. Eksp. Theor. Fiz 57, 1128 (1969) [Sov. Phys. JETP 30, 616 (1970)].

[7] For a review, see J. J. O'Dwyer, The Theory of the Dielectric Breakdown of Solids (Oxford University Press, London, 1964).

[8] Guiliano, C. R. and Marburger, J. H., Phys. Rev. Lett. 27, 905 (1971).

[9] Von Hippel, A., J. Appl. Phys. 8, 815 (1937).

10] Akhmanov, S. A., Sukhorukov, A. P., and Khokhlov, R. V., Sov. Phys. Usp. 10, 609 (1968).

11] Bloembergen, N., private communication.

12] Alcock, A. J., DeMichelis, Claudio, and Richardson, M. C., IEEE J. Quantum Elec. QE-6, 622 (1970).

[13] Bass, M. and Barrett, H. H., IEEE J. of Quantum Elec. QE-8, 338 (1972).

[14] Zverev, G. M., Mikhailova, T. N., Pashkov, V. A., and Solov'na, N. M., Zh. Eksp. Theor. Fiz. 53, 1849 (1967). [Sov. Phys. JETP 26, 1053 (1968).]

[15] Yablonovitch, E., Thesis, Harvard University (1972).

[16] Kuchin, V. D., Rep. Akad. Sci. USSR, 114, 301 (1957); Sov. Phys. Solid State, 1, 405 (1959).

[17] Watson, D. W., Heyes, W., Kao, K. C., and Calderwood, J. H , IEEE Trans Elec. lus. El-1, 30 (1965). Also, Vorob'ev, G. A. Lebedeva, N. I. , and Naderova, G. S., Fizika Tverdogo Tela, 13, 890 (1971), [Sov. Phys. Solid State, 13, 736 (1971)].

[18] Giuliano, C. R., to be published.

[19] Wang, Chen-Show, Phys. Rev. 173, 908 (1968).

[20] Born, M. and Wolf, E., Principles of Optics, (Pergamon Press, Inc., New York, 1959).

[21] Talanov, V. I., Zh. Eksperim, i. Theor. Fiz. Pis'ma Redaktsiyu 2, 218 (1965) [Sov. Phys. JETP Letters 2, 138 (1965)].

[22] Dawes, E. L., and Marburger, J. H., Phys. Rev. 179, 862 (1969).

[23] Kerr, E. K., IEEE J. Quantum Elec. QE-6 616 (1970).

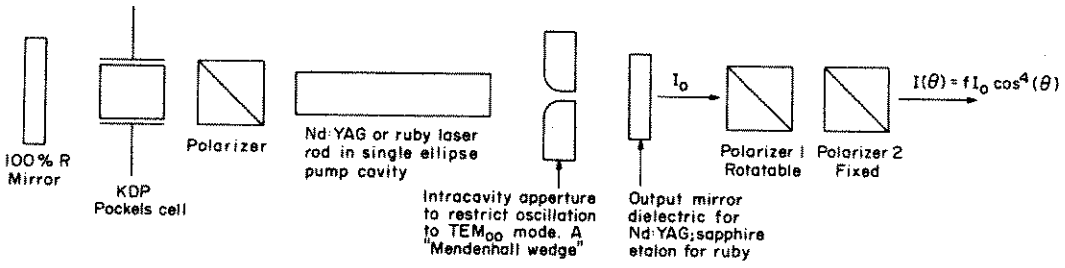

Figure 1. Laser and variable attenuator configuration for damage studies.

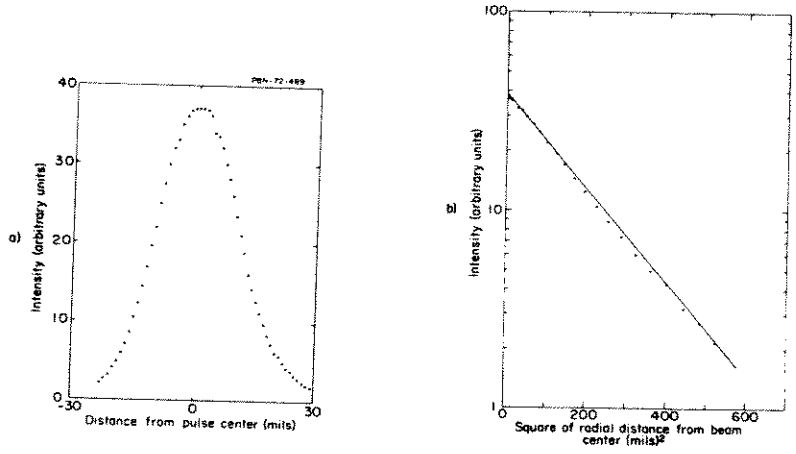

Figure 2. Intensity disbribution of the YAG laser as a function of radial distance from the beam center at the position of the focusing lens. (a) The data was taken by sweeping a 1-mil aperture through the beam with each data point corresponding to a different laser shot. A small dip near the center could not be reproduced and indicates the experimental errors in the measurement. (b) By plotting the log of the intensity as a function of the radial distance squared, it was found that the output beam has a Gaussian profile $[-2r^2/\sigma^2]$ where σ is measured to be 0.485 ± 0.005 millimeters.

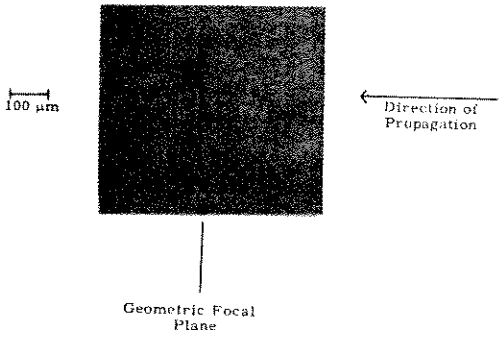

Figure 3. Intrinsic damage in RbCl. Damage which we have considered to be intrinsic had this basic shape in all the materials tested.

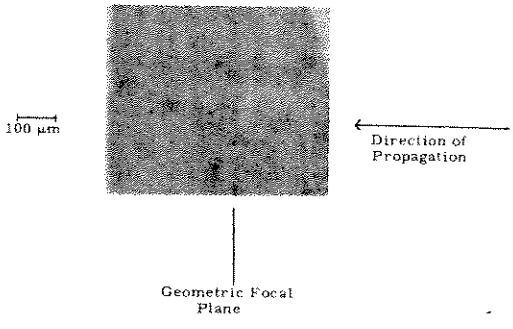

Figure 4. Inclusion damage in RbCl.

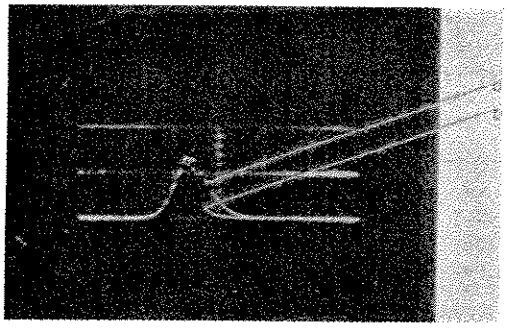

Figure 5. Nd:YAG laser pulse transmitted through the sample. (a) No damage produced. (b) Damage produced at or just before the pulse reached its maximum intensity. These were two successive pulses in the same volume. Note that there is no evidence that the second pulse, the one which produced damage, is any different from the rest.

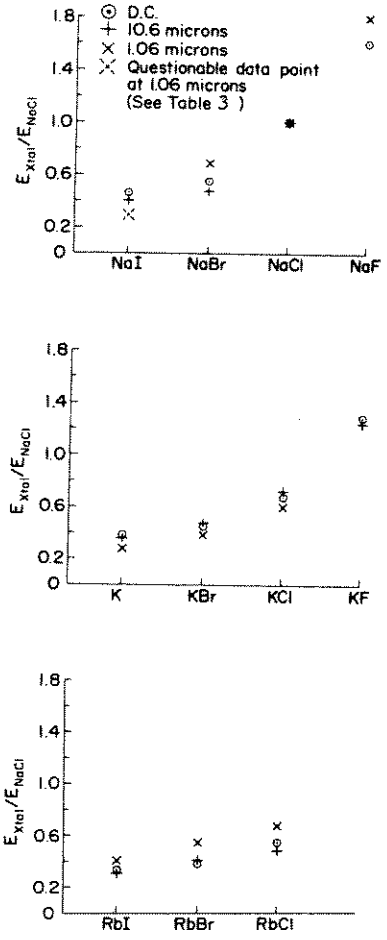

Figure 6. Comparison of breakdown strengths for various alkali halides studied at dc, 10.6 microns, and 1.06 microns. Values for 10.6 and 1.06 microns are root-mean-square field strengths and not peak fields. The data at dc is taken from reference 9 and the 10.6 micron data is taken from reference 4. (a) Relative breakdown fields for Na salts normalized to E_{NaCl}. (b) Relative breakdown fields for K salts normalized to E_{NaCl}. (c) Relative breakdown fields for Rb salts normalized to E_{NaCl}.

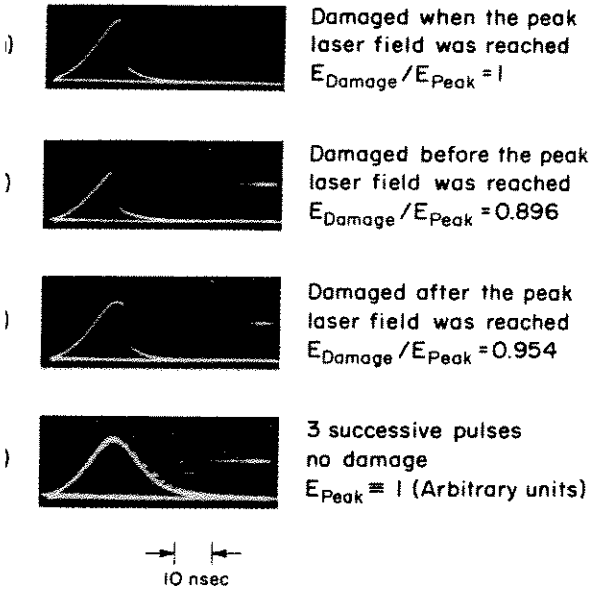

igure 7. Ruby laser pulses transmitted through NaCl sample.